AD-A177 583 AN EXPERIMENTAL STUDY OF THE DYNAMIC MECHANICAL PROPERTIES OF AN AL-SIC(W) COMPOSITE(U) BROWN UNIV PROVIDENCE RI DIV OF ENGINEERING A MARCHAND ET AL. 1/1

UNCLASSIFIED DEC 86 N00014-85-K-0687 F/G 11/4 NL

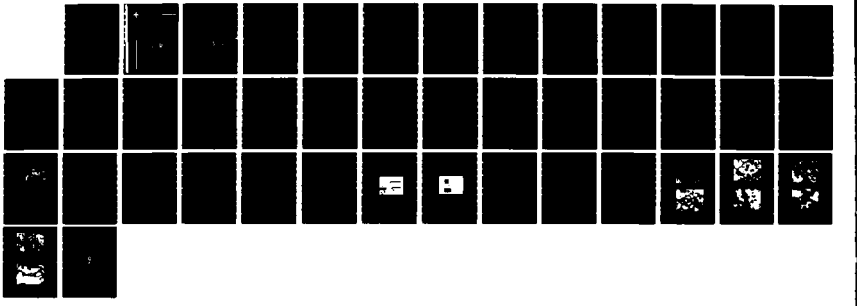

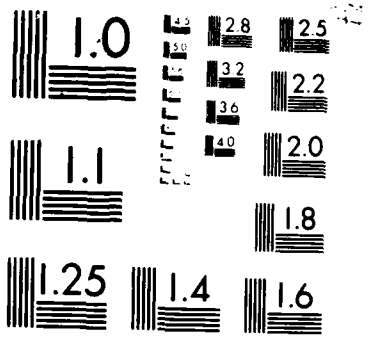

MICROCOPY RESOLUTION TEST CHART

Brown University
DIVISION OF ENGINEERING
PROVIDENCE, R.I. 02912

AN EXPERIMENTAL STUDY OF THE DYNAMIC MECHANICAL PROPERTIES OF AN Al-SiC_W COMPOSITE

by

A. Marchand, J. Duffy, T.A. Christman and S. Suresh
Division of Engineering
Brown University
Providence, R.I. 02912

Brown University
Division of Engineering
Providence, R.I. 02912

AN EXPERIMENTAL STUDY OF THE DYNAMIC MECHANICAL PROPERTIES OF AN Al-SiC_W COMPOSITE

by

A. Marchand, J. Duffy, T.A. Christman and S. Suresh
Division of Engineering
Brown University
Providence, R.I. 02912

Brown University Technical Report
ONR-SDIO N00014-85-K-0687/1

December, 1986

December, 1986

An Experimental Study of the Dynamic Mechanical Properties of an Al-SiC_w Composite

by

A. Marchand, J. Duffy, T.A. Christman, and S. Suresh
Division of Engineering
Brown University
Providence, Rhode Island

Abstract

This report presents initial results of an experimental study of the dynamic deformation and dynamic fracture behavior of a 2124-T6 aluminum alloy reinforced with 13.2 v/o SiC whiskers. Results are compared with the quasistatic behavior and with the behavior of the unreinforced 2124-T6 aluminum alloy. Two types of tests are described, one to provide static and dynamic stress-strain curves of the material in shear and the other to measure static and dynamic values of the critical stress intensity factors, K_{Ic} and K_{Id}, for tensile fracture. Results show that the presence of the reinforcing whiskers raises the dynamic and static flow stress of the material in shear. It is also evident that the reinforced material has considerably more ductility in shear than it has in axial deformation. As expected, the fracture response, as measured by the critical stress intensity factor K_{Ic}, is not as favorable for the reinforced material as for the unreinforced. However, dynamic loading raises the value of K_{Ic} for the reinforced material while producing almost no change in the unreinforced. For the reinforced material, the rate of loading is important in determining toughness, as measured by the value of K_I, but has little influence on the stress-strain behavior in shear.

1. Introduction

For many materials, mechanical behavior can be quite different under dynamic as opposed to static loading [1-5]. Thus, to design for resistance to impact loading, to dynamic penetration or for other dynamic conditions, it is important to know the dynamic stress-strain and the dynamic fracture behavior of the material in question. The present report describes tests of this nature performed with specimens of 2124-T6 aluminum alloy reinforced with 13.2 v/o SiC whiskers, as well as with the unreinforced aluminum alloy.

For published information on the quasi-static mechanical properties of Al/SiC_w composite, the reader is referred to recent papers [6,7] and to the review by Nair et al [8] which includes fracture behavior, stress-strain behavior in tension, compression and shear, as well as fatigue and creep properties. Studies have also been performed on the role of the matrix, of the whisker and of the interfacial bond on overall composite behavior [9]. Dynamic behavior, however, has received very little attention although it is of significant interest in numerous applications. Two different dynamic tests are described in the present report, both of which make use of the principles of the Kolsky bar (split-Hopkinson bar). The first set of tests is intended to study dynamic fracture initiation and the second the dynamic stress-strain behavior of the material.

In many investigations, fracture behavior is evaluated by means of the Charpy test, mainly because of its low cost, convenience and familiarity. However, Charpy test results are difficult to relate to fracture mechanics concepts and, in particular, to the stress intensity factor, K_I. More fundamental difficulties with the Charpy test lie in the fact that plane strain conditions are not fully met in the specimen, and that the wave pattern within the specimen is complex, so that it is not possible to determine the stress state at the crack tip at the instant of fracture initiation. Accordingly, at Brown University we introduced a new fracture test [10], with which

one can attain a stress intensity factor rate above 10^6 MPa$\sqrt{m}$/s and in which plane strain conditions are met. This is achieved by propagating a sharp-fronted tensile pulse along a cylindrical specimen containing a fatigue pre-crack, the tensile pulse being initiated by an explosive charge. Instrumentation provides a measure of the average stress at the fracture site and of the crack opening displacement, both as functions of time. For ductile materials, as in the present instance, the resulting data are used to evaluate a critical J-integral for the test and an equivalent critical stress intensity factor. While this experimental technique is relatively new, it has been employed previously to study the fracture initiation behavior of a number of steels [11-13]. A detailed finite element analysis has also been conducted of this test using the specific geometry and incoming wave form [14]. The results of the analysis indicate that the values of the equivalent critical stress intensity factor obtained by means of this test are reliable, in brittle or ductile fracture.

In the second series of tests, the dynamic stress-strain behavior of the material is determined in shear by means of a torsional Kolsky bar. With this apparatus a strain rate on the order of 10^3/s is imposed on the specimen, as compared with 10^{-4}/s achieved in a conventional quasi-static test. In view of the anisotropic nature of the composite material, an evaluation of the dynamic tensile properties would be of great interest. To date, however, the Kolsky bar has been employed almost exclusively in compression and in torsion, because no fully satisfactory tensile test method has been devised to impose high strain rates in tension which gives reliable values of stress and strain in the specimen. One should note that the highest strain rate attainable in a programmable servo-hydraulic testing machine is about 10/s. If higher rates are attempted with such a loading machine, then stress pulses will propagate up and down the loading column making it impossible to obtain even approximate measurements of load or deformation in the specimen. Static tests have also been performed with the present material both in shear and in tension.

Materials Tested

The materials tested are 2124-T6 aluminum alloy either reinforced with 13.2 v/o SiC whiskers or unreinforced. Properties of these materials, as given in the literature, are presented in Table 1. Results of chemical analyses for the reinforced and unreinforced materials are given in Table 2, which indicates some variation between the two materials. Similar variations have been observed previously [15]. Extruded cylindrical rods of both materials were purchased from ARCO Corporation. As is evident from Table 1, the potential advantages of the composite as regards mechanical behavior lie in its higher Young's modulus and higher flow stress, while its disadvantage lies in the low ductility shown in the third line. The composite consists of a P/M 2124 aluminum alloy matrix, with SiC whiskers added. Initially, the whiskers have an aspect ratio of about 100 with a length up to 50 microns. When first added to the material their orientation is random. However, for bar stock, as a result of the manufacturing process which includes extrusion, the whiskers tend to take a preferred orientation along the axis of the bars, and are also considerably shortened due to breakage.

The material is tested in the as-received condition, i.e. aged by ARCO to the T-6 condition. However, the aging time is based on the peak in the hardness of the unreinforced aluminum alloy. Related studies of aging time treatment were performed with plate stock of the same chemically composition as the bar stock used in the studies of mechanical behavior. These studies included a determination of the matrix microhardness as a function of aging time, and showed that aging of the reinforced material for the same length of time as the unreinforced material results in overaging of the matrix in the reinforced material, Figure 1. In addition, tensile tests were performed with standard tensile specimens machined from the plate stock. These show that at quasi-static rates the influence of aging time on the tensile stress-strain behavior is not very strong, Figures 2(a) and 2(b), as compared with the

normal variation in stress-strain behavior due to material processing. Static tensile tests were also performed with standard specimens machined from extruded bar stocks material, both reinforced and unreinforced. The static curves presented in Figure 3 indicate that the presence of the whiskers increases the ultimate stress from 538 MPa for the unreinforced to 728 MPa for the reinforced. There is also a substantial increase in strength and in fracture strain as compared with results of tests performed with specimens taken from plate stock. These differences are probably due to the differences in processing of these materials, and have also been observed by Chellman [16].

Standard Charpy impact tests were performed with specimens of both the reinforced and unreinforced materials. These indicate that the Charpy energy for the unreinforced material is 14 joules while for the reinforced it drops to 1.4 joules.

Description of the Dynamic Stress-Strain Experiment

The dynamic test we employ to determine stress-strain behavior is an adaptation of Kolsky's split-Hopkinson bar [17]. In Kolsky's original test a penny-shaped specimen was loaded in compression by an elastic incident pulse initiated through an explosive detonation at one end of the bar. Records were obtained of the pulses incident, reflected from and transmitted through the specimen. As was shown by Kolsky, the reflected pulse provides a measure of the average strain rate in the specimen as a function of time, while the transmitted pulse provides a measure of corresponding values of stress. An integration of the former gives strain as a function of time, and elimination of time between stress and strain records yields a stress-strain curve for the material at a known strain rate.

In our adaptation of the Kolsky bar the specimen is deformed in torsion. For this purpose, it is shaped as a thin-walled tube machined with heavy flanges for attachment to the torsional bar, Figure 4. The pulse can be initiated through explosive loading [18] but, in the present tests, a stored torque is used for this purpose [19]. This torque is stored at the left end of the bar between the torque pulley and the clamp, Figure 5(a). To obtain a sharp-fronted stress pulse, rapid release of the clamp is essential and this is effected by the fracture of a brittle breaker piece. By this method, strain rates in shear on the order of 10^3/s can be imposed on the specimen. The incident and transmitted pulses are recorded by strain gages mounted at 45° to the axis of the bar, Figure 5(b), and interpretation of the shear strain records follows that given by Kolsky for axial loading, mutatis mutandis. This torsional apparatus has been used frequently to study the stress-strain behavior of a number of metals over a range of temperatures and under different loading conditions [20-22]. Static stress-strain curves are obtained in the same apparatus with similar specimens by loading statically through the right end of the bar against the clamp.

Results of Dynamic Stress-Strain Tests in Shear

For the 2124-T6 aluminum alloy, results for the reinforced and unreinforced material are presented in Figures 6 through 8. In these tests, loading was applied in a direction perpendicular to the orientation of the majority of the whiskers in the reinforced material, and until complete fracture of the specimens. It may be noted that the stress is always higher for the whisker reinforced material; also that the ductility is considerably greater in shear than the nominal ductility in tension given in Table 1, and that it increases with strain rate. In the range tested, it appears that strain rate has only a small effect on the flow stress level in the case of specimens machined from one bar of the composite (labeled Z1) and no effect for specimens taken from another bar (Z2). These results are summarized in Tables 3 and 4. The strengthening due to the presence of whiskers is given in Table 3, in which τ_{uc} and τ_{um} represent, respectively, the ultimate shear stress in specimens of the aluminum alloy with and without whisker reinforcement. It is evident from this table that the strengthening effect of the whiskers varies from one bar to another presumably because of differences in material or manufacture. In general, however, the ultimate shear stress in the composite is about 20% greater than in the 2124-T6 aluminum alloy.

The influence of whisker reinforcement on ductility in shear, i.e. on the fracture strain in shear, is to reduce it from about 45% to 30% in quasistatic loading. In this respect, the difference between bars Z1 and Z2 is insignificant. For dynamic deformation there is also some reduction but it appears to be less pronounced. The influence of strain rate on the stress level of the unreinforced material is approximately what one would expect for an aluminum alloy, since, in general, the strain rate sensitivity of aluminum depends on its purity, at least in the strain rate range from the quasi-static to $10^3 s^{-1}$ where high purity aluminum shows a high strain rate sensitivity and aluminum alloys a low sensitivity [23]. Based on these results

only a small strain rate sensitivity can be expected in the stress-strain behavior of a 2124 aluminum alloy.

The strain hardening rate of the material appears to be independent of strain rate, in the range of the present tests, and almost the same for the matrix as for the whisker reinforced material. In either case the stress-strain curves can be fitted by a power law of the form

$$\tau/\tau_y = (\gamma/\gamma_y)^m$$

where τ_y and γ_y represent values of stress and strain at first yield and where m is a constant. For values of strain greater than 2%, m = 0.17 for the unreinforced aluminum alloy and 0.16 for the whisker reinforced. As far as strain rate sensitivity is concerned, here again there appears to be some difference in the behavior of the material taken from bars Z1 and Z2, but in neither case is strain rate sensitivity of particular consequence in this range of strain rates. This result is consistent with the generally accepted behavior of aluminum alloys [23, 24].

Description of the Dynamic Fracture Initiation Experiment

For the dynamic fracture test, Figure 9, the specimen consists of a notched round bar 2.54 cm in diameter and about 116 cm long. As mentioned previously, a circumferential notch is machined around the bar about 77 cm from its loading end, and a fatigue crack is grown in at the root of this notch [10]. Since it is essential that the fatigue crack grow concentrically, a specially constructed apparatus is used for this purpose [11]. It consists of a rotating beam placed in bending by imposing a fixed displacement at its midpoint, Figure 10. The resulting notched section is shown in Figure 11.

During the dynamic fracture test, the loading pulse is initiated at the end of the bar by the detonation of an explosive charge placed against a loading head and arranged so that the initial pulse propagating down the bar is one of tension, Figure 9. Fracture is produced when this tensile pulse reaches the fatigue precracked section. In evaluating the stress, data reduction follows Kolsky's original method since the transmitted portion of the incident pulse is proportional to the load carried at the fracture site and hence provides a measure of average stress at the fracture site as a function of time. As may be seen in Figure 12, loading to fracture takes about 10 or 15 microseconds. The loading pulse which is incident on the fracture site is given an amplitude considerably greater than that of the transmitted pulse, to insure that fracture always occurs on a rising load. Crack opening displacement (COD), or more precisely a notch opening displacement, is measured optically by an adaptation of the moire technique. For this purpose a glass slide spans the notch and is cemented to the bar on one side of the notch. A grid of 32 lines per mm is printed on the glass slide and a like grid is deposited on the metal surface covering an area previously polished to a mirror finish. During a test a powerful light emanating from a fiber optic tube is directed through the glass slide and reflected from the metal surface to a photodiode. Relative motion between the slide and the

metal surface creates an alternating light-dark pattern detected by the photodiode to produce a trace on an oscilloscope screen. Since a pair of these optical gages is used, one on each side of the bar, two traces are obtained, Figure 13.

The method employed for data reduction depends in general upon the degree of ductility of the material tested. In view of the high ductility of the present aluminum alloys, whether reinforced or unreinforced, the fracture does not meet the requirement for a valid K_{Ic} test as expressed by

$$R \geq 2.5 \, (K_{Ic} \, \sigma_y)^2 \tag{1}$$

where R is the radius of the unfractured ligament and σ_y the yield stress of the material at a strain rate comparable to that attained near the root of the notch. As a result, a J integral approach must be adopted. The criterion suggested by Paris [25] for a valid J_{Ic} test and the one adopted in evaluating present results is

$$R \geq 50 \, J_{Ic} \, \sigma_y \tag{2}$$

As shown by Rice et al [26] for a notched round bar the value of J may be determined from a load-displacement curve by employing

$$J_{dc} = \frac{1}{2\pi c^2} \left[3 \int_0^{\delta} P d\delta - P\delta \right] \tag{3}$$

where P is the transmitted force, δ the load-point displacement due to the presence of the crack and c the radius of the uncracked ligament. This expression for J_d, is convenient in the present instance since it is expressed in terms of P, δ, and c, all of which are determined in the experiment, if the notch opening is taken as the value of δ.

Nakamura, et al. [27] made a detailed finite element study of the present fracture experiment and calculated J using a rigorous expression based on the energy

flux into the moving crack tip and including dynamic effects. They also evaluated J_{Id}, based on Equation (3). The finite element grid employed in the calculation is shown in Figure 14, which gives the appearance of the grid during passage of the stress pulse. The elastic-plastic constitutive relation employed is that of mild steel deforming dynamically and the loading pulse is given the shape seen in the experiment. The principal conclusion of the analysis is that the difference between the value of J_d based on the expression for load-deflection, Equation (3), and the rigorous value of J is small when the notch is sufficiently deep. In view of this conclusion the experimental technique was modified so the depth of the notch in the present specimens is always greater than 60% of the radius of the bar, leading to an error of less than 10%. In addition, Nakamura et al showed that a Mode I plane strain field obtains at the crack-tip and that notch-opening constitutes a good measure of load-point displacement. Finally, they showed that at the instant of fracture initiation the effective stress field is symmetric to either side of the fracture plane. This includes both normal and shear components of stress in the neighborhood of the crack tip. Thus, the advantages of the present test are that it provides rapid loading simultaneously with accurate measures of average stress and of notch opening, leading to a reliable value of J at fracture initiation. In the experiments an equivalent stress intensity factor K_I is calculated from

$$K_I^2 = \frac{E J_{Ic}}{1 - \nu^2}$$

where E and ν are elastic constants of the specimen material.

Quasi-static fracture initiation tests are also performed for purposes of comparison. The specimen employed has the same geometry as does the dynamic specimen, except that its overall length is only 71 cm. The materials for the static, fracture test, the

Charpy Test and the dynamic and static plasticity tests were taken from previously-tested dynamic fracture specimens, Figure 15. It should be noted that the material outside the fracture zone remains elastic in both the static and dynamic tests. For the static test, as in the dynamic, a circumferential notch is machined and a fatigue crack grown at the root of this notch. The load is measured to provide average stress at the fracture site. Notch opening displacement again is measured optically. However, for the static tests an MTI Photonic Sensor is employed.

Results of the Fracture Initiation Tests

Typical curves showing load as a function of COD for the reinforced and unreinforced material are shown in Figure 16 for two dynamic tests and one static test. The dimension a in the figure refers to the depth of the fatigue crack. Although there is some difference between results in the two dynamic tests, this difference is not as large as appears at first, because the unfatigued ligament is greater for the upper curve. Calculated values of the critical stress intensity factors K_{Ic} for static loading and of K_{ID} for dynamic, are given in Table 5. values Three tests were performed in each case but only the average is reported. It appears that the reinforced material is not as tough as the aluminum alloy, the drop in the critical values of K_I being almost 50%. It appears also that under dynamic loading the fracture toughness of these materials is somewhat greater than statically.

The microscopic features of the fracture surfaces obtained in the dynamic tests are shown in Figures 17-19. Figures 17a and 17b are scanning electron micrographs of the fatigue area, whereas Figures 18 and 19 show the fractography in the dynamic fracture initiation and growth regimes, respectively. Predominantly fibrous fracture with clear evidence of whisker pull out can be noticed in these figures. Figure 20 provides the microscopic details of quasi-static fracture in the composite at 0° and 45° tilt. These preliminary observations seem to indicate no significant differences in the failure mechanisms between dynamic and static tests at room temperature. Further detailed analyses of the failure mechanisms are currently in progress. We are also carrying out a comprehensive TEM investigation of microstructural development, aging kinetics and failure modes in commercial and binary (Al-4% Cu) aluminum alloys with and without SiC reinforcement. It is hoped that the results of this parallel study will provide valuable insights into the microscopic mechanisms of failure in the aging program on the dynamic behavior of metal-matrix composites.

Conclusions

A series of experiments has been conducted to determine the dynamic fracture initiation behavior and dynamic stress-strain behavior of a metal-matrix composite: 2124-T6 aluminum reinforced with silicon carbon whiskers. The dynamic fracture tests are performed with prefatigued notched round bars in which the notched section is loaded by an explosively initiated tensile pulse. The stress-strain behavior is determine in shear in a torsional Kolsky (split-Hopkinson) bar. In general, the results show that fracture toughness in the reinforced material is sensitive to loading rate but that the stress-strain behavior does not change with deformation rate in the range from a quasi-static strain rate to 3000/s.

Results of the fracture initiation tests give a critical dynamic stress intensity factor of about 27 MPa$\sqrt{m}$ for the reinforced material compared with a value of 41 MPa$\sqrt{m}$ for specimens of the 2124-T6 aluminum alloy matrix. These values are somewhat greater than corresponding values of the stress intensity factor for quasi-static fracture initiation which are 21 MPa$\sqrt{m}$ for the reinforced material and 37 MPa$\sqrt{m}$ for the unreinforced.

The stress-strain curves show only a small strain rate sensitivity either for the reinforced or for the unreinforced materials. However, the reinforced material is considerably stronger in shear than the unreinforced both statically and dynamically. Results also show a considerably greater ductility in shear than in tension.

Additional experiments are needed with this material to determine the influence of the percent whisker inclusion and of test temperature on the fracture initiation and stress-strain behavior. Additional microscopic observations of the fracture surfaces are needed to ascertain the dominant fracture mode as it depends on loading rate, test temperature, the type of fracture test and the constitution and composition of the aggregate.

ACKNOWLEDGEMENTS

The research support of the Office of Naval Research, Structural Mechanics Program, under ONR-SDIO grant N00014-85-K-0687 is gratefully acknowledged. Thanks are also due to Mr. George LaBonte for his help in carrying out the experiments.

REFERENCES

1. J. Duffy, "The Dynamic Plastic Deformation of Metals: A Review, "Technical Report Air Force Wright Aeronautical Laboratories; AFWAL-TR-82-4024, October, 1982.

2. K. Kawata and J. Shioiri (eds.), High Velocity Deformation of Solids, IUTAM Symposium, Tokyo, Japan, 1977.

3. U.S. Lindholm and R.L. Bessey, "A Survey of Rate Dependent Strength Properties of Metals," Technical Report AFML-TR-69-119, April 1969.

4. J.A. Zukas, T. Nicholas, H.F. Swift, L.B. Greszczuk, and D.R. Curran, Impact Dynamics Wiley & Sons, 1982.

5. J. Harding (ed.), Mechanical Properties at High Rates of Strain, 1984, Proc. Third Conf. on Mechanical Properties of Materials at High Rates of Strain, Oxford, 1984.

6. A.P. Divecha, S.G. Fishman and S.D. Karmarkar, "Silicon Carbide Reinforced Aluminum - A Formable Composite," Journal of Metals, Sept. 1981, Vol. 33, pp 12-17.

7. D.L. McDanels, "Analysis of Stress-Strain, Fracture and Ductility Behavior of Aluminum Matrix Composites Containing Discontinuous Silicon Carbide Reinforcement," Met. Trans. A, Vol. 16A, June 1985, pp 1105-1115.

8. S.V. Nair, J.K. Tien and R.C. Bates,"SiC Reinforced Aluminum Metal Matrix Composites - A Review," Int. Met. Rev., Vol. 30, No. 6, 1985, pp 275-290.

9. H.J. Rack, T.R. Baruch and J.L. Cook, "Mechanical Behavior of Silicon Carbide Whisker Reinforced Aluminum Alloys," in Progress in Science and Engineering of Composites, Edited by T. Hayashi, K. Kawata and S. Umekawa, ICCM-IV, Tokyo, 1982, pp 1465-1471.

10. L.S. Costin, J. Duffy and L.B. Freund, "Fracture Initiation in Metals Under Stress Wave Loading Conditions," in Fast Fracture and Crack Arrest, Edited by G. Hahn and M.F. Kanninen, ASTM STP 627, American Society for Testing and Materials, Philadelphia, pp. 301-318.

11. L.S. Costin and J. Duffy, "The Effect of Loading Rate and Temperature on the Initiation of Fracture in a Mild, Rate-Sensitive Steel," Trans. of ASME, Vol. 101, Journal of Engineering Materials and Technology, July, 1979, pp. 258-264.

12. M.L. Wilson, R.H. Hawley and J. Duffy, "Strain Rate and Strain Rate History Effects in Two Mild Steels," Brown University Report NSF ENG 75-18532/8, March, 1979.

13. H. Couque, J. Duffy and R.J. Asaro, "Correlation of Microstructure with Dynamic and Quasi-Static Fracture of a Plain Carbon Steel", presented at Golden Gate Conference on Metals and Welding, San Francisco, California, 1985.

14. T. Nakamura, C.F. Shih, and L.B. Freund,"Elastic-Plastic Analysis of a Dynamically Loaded Circumferentially Notched Round Bar," Engineering Fracture Mechanics, Vol. 22, No. 3, pp 437-452, 1985.

15. T.E. Scott, unpublished results, Michigan Technological University, Houghton, Michigan.

16. D.J. Chellman,"SiC/Al for High Performance Aircraft," Golden Gate Metals and Welding Conference, San Francisco, California, February 9-11, 1983.

17. H. Kolsky, "An Investigation of the Mechanical Properties of Materials at Very High Rates of Loading," Proc. Phys. Soc., London, 1949, 62-B, 676.

18. J. Duffy, J.D. Campbell and R.H. Hawley, "On the Use of a Torsional Split Hopkinson Bar to Study Rate Effects in 1100-0 Aluminum", Journal of Applied Mechanics, March, 1971, pp. 83-91.

19. P.E. Senseny, J. Duffy and R.H. Hawley, "Experiments on Strain Rate History and Temperature Effects during the Plastic Deformation of Close-Packed Metals," Journal of Applied Mechanics, March, 1978, pp. 60-66.

20. A.M. Eleiche and J. Duffy, "The Effects of Temperature on the Static and Dynamic Stress-Strain Characteristics in Torsion of 1100-0 Aluminum," International Journal of Mechanical Sciences, Vol. 17, February, 1975, pp. 85-96.

21. C.Y. Chiem and J. Duffy, "Strain Rate History Effects and Observations of Dislocation Substructure in Aluminum Single Crystals following Dynamic Deformation," Materials Science and Engineering, Vol. 57, No. 2, 1983, pp. 233-247.

22. S. Tanimura and J. Duffy, "Strain Rate Effects and Temperature History Effects for Three Different Tempers of 4340 VAR Steel," International Journal of Plasticity, Vol. 2, 1986, pp. 21-35.

23. D.L. Holt, S.G. Babcock, S.J. Green and C.J. Maiden, "The Strain Rate Dependence of the Flow Stress in Some Aluminum Alloys," Trans. ASM, Vol. 60, 1967, pp 152-259.

24. R.W. Klopp, R.J. Clifton and T.G. Shawki, "Pressure-Shear Impact and the Dynamic Viscoplastic Response of Metals," Mechanics of Materials, Vol. 4, 1985, pp 375-385.

25. P.C. Paris, written discussion of J.A. Bealey and J.D. Landes, "The J-Integral as a Fracture Criterion," Fracture Toughness ASTM, STP 514, American Society for Testing and Materials, Philadelphia, 1972, pp 1-23.

26. J.R. Rice, P.C. Paris and J.C. Merkle, "Some Further Results of J-Integral Analysis and Estimates," Progress in Flaw Growth and Fracture Toughness Testing, ASTM STP 536, pp 231-245, American Society for Testing and Materials, Philadelphia (1973).

27. T. Nakamura, C.F. Shih and L.B. Freund, "Elastic-Plastic Analysis of a Dynamically Loaded Circumferentially Notched Round Bar," Engineering Fracture Mechanics, Vol. 22, No 3, 1985, pp 437-452.

C:COMPOSI2.wp
12/16/86 lmp

Table 1

TENSILE PROPERTIES OF THE MATERIALS STUDIES

(Values supplied by ARCO Chemical Company)

	2124 - T6 Aluminum Alloy	2124-T6 Aluminum Alloy Reinforced with 13.2 w/o SiC_w
Elastic Modulus, E (G Pa)	69	(L) 96
Yield Stress, σ_y (M Pa)	300	(L) 500
Maximum Elongation (%)	25	(L) 2
Poisson's Ratio, γ	0.33	(L) 0.28

TABLE 2

CHEMICAL COMPOSITION (Weight %)

	13.2 v/o SiC 2124-Al	2124-Al
Carbon	4.33%	0.014%
Copper	3.41%	4.10%
Iron	0.02%	0.02%
Magnesium	1.88%	1.92%
Manganese	0.24%	0.49%
Molybdenum	0.001%	0.001%
Nickel	-----	----
Silicon	9.88%	0.006%
Sulfur	0.0033%	0.0034%
Titanium	----	0.002%
Vanadium	0.001%	----
Zirconium	----	----
Aluminum	Balance	Balance

Table 3 The influence of whisker reinforcement on shear strength

Specimen	Shear Strain Rate (s^{-1})	10^{-4}	900	1300	1600	3500
W	Ultimate Strength in Shear of Aluminum Alloy τ_{um} (MPa)	315	295	300	310	305
Z1	Ultimate Strength in Shear of Whisker Reinforced Aluminum τ_{uc} (MPa)	390	335	365	375	375
	$\Delta = 100\ (\tau_{uc} - \tau_{um})/\tau_{um}$	24	14	21	21	23
Z2	Ultimate Strength in Shear of Whisker Reinforced Aluminum τ_{uc} (MPa)	382	-	-	381	388
	$\Delta = 100\ (\tau_{uc} - \tau_{um})/\tau_{um}$	21	-	-	23	27

Table 4 The influence of the whisker reinforcements on ductility in shear - (Ductility is approximately equal in bars Z1 and Z2)

Shear Strain Rate (s^{-1})	10^{-4}		900		1300		1600		3500	
SiC vol (%)	0	13.2	0	13.2	0	13.2	0	13.2	0	13.2
Ductility (%)	44	29	38	35	52	38	50	40	50	40

Table 5 Static and Dynamic Values of the Critical Stress Intensity Factor During Fracture Initiation at Room Temperature

Stress Intensity Factor ($MPa\sqrt{m}$)	Stress Intensity Rate ($MPa\sqrt{m}/s$)	Material	
		2124-T6 Aluminum Alloy Matrix	2124-T6 Aluminum Alloy with 13.2v/o SiC Whiskers
K_{Ic}	$\dot{K}_{Ic} = 1$	37 ± 2	21 ± 1
K_{Id}	$\dot{K}_{Id} = 2 \times 10^{6}$	41 ± 2	27 ± 1

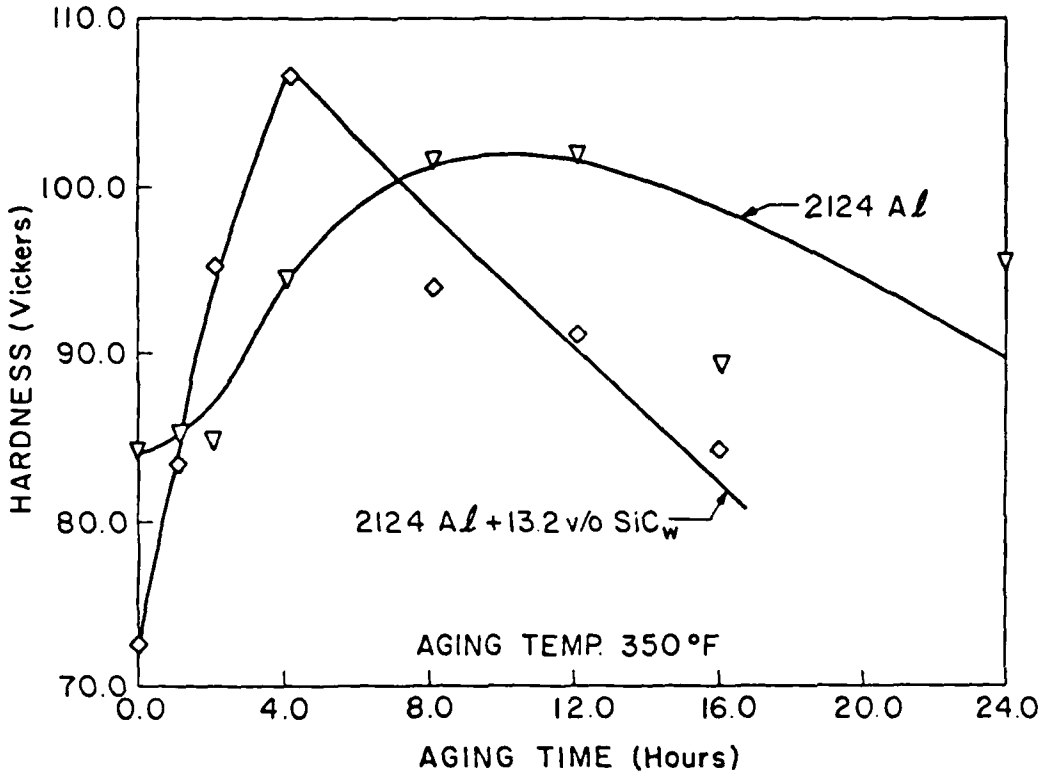

FIGURE 1. MICROHARDNESS OF THE MATRIX MATERIAL AS A FUNCTION OF AGING TIME.

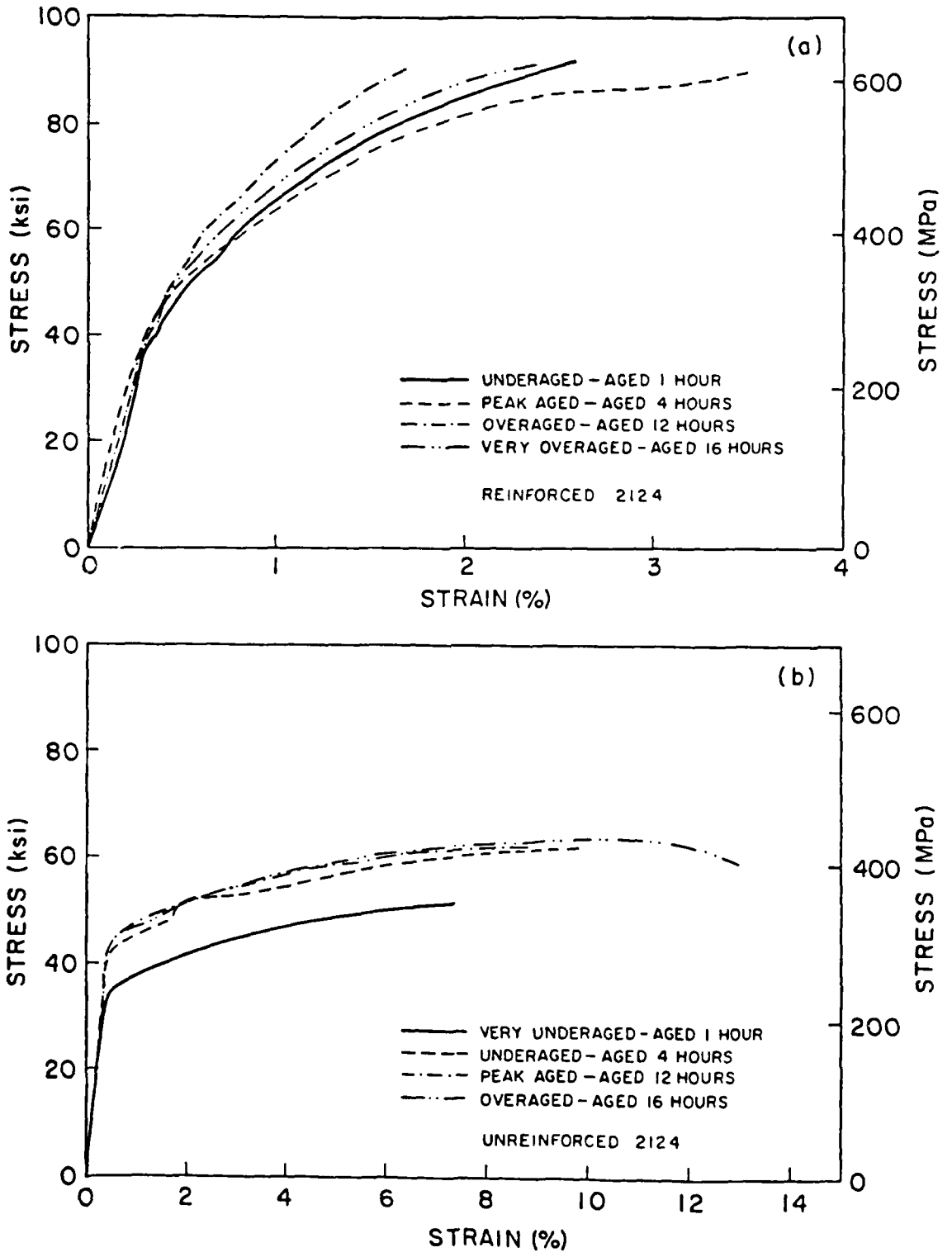

FIGURE 2. INFLUENCE OF AGING TIME AT 350° F ON THE STRESS-STRAIN BEHAVIOR IN TENSION. SPECIMENS ARE TAKEN FROM PLATE STOCK.

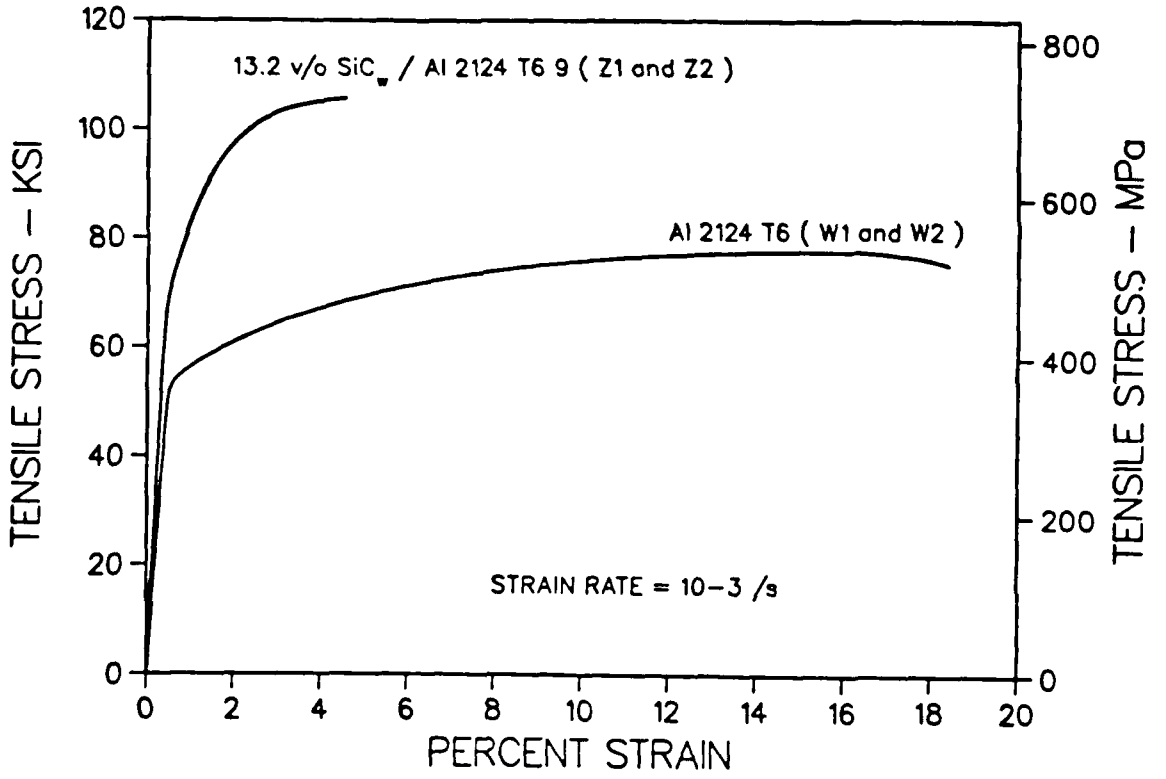

FIGURE 3. QUASI-STATIC STRESS-STRAIN BEHAVIOR IN TENSION. SPECIMENS ARE TAKEN FROM 25mm DIAMETER EXTRUDED BAR.

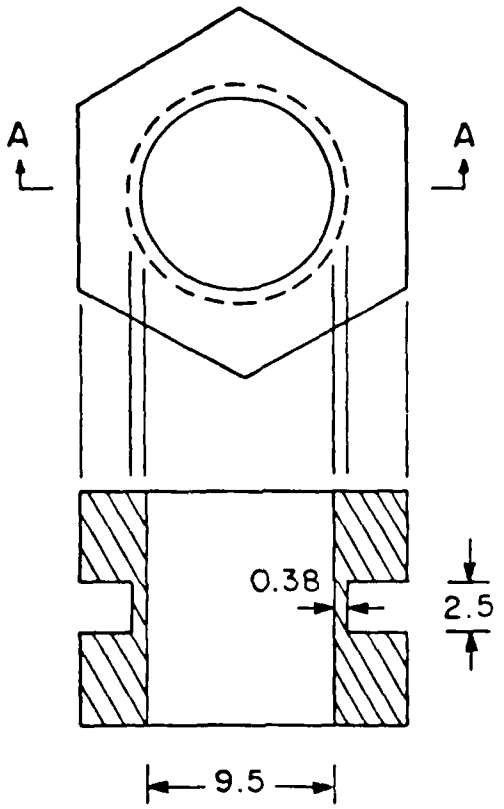

FIGURE 4. DETAILS OF TORSIONAL SPECIMEN WITH HEXAGONAL MOUNTING FLANGES. DIMENSIONS ARE IN MILLIMETERS.

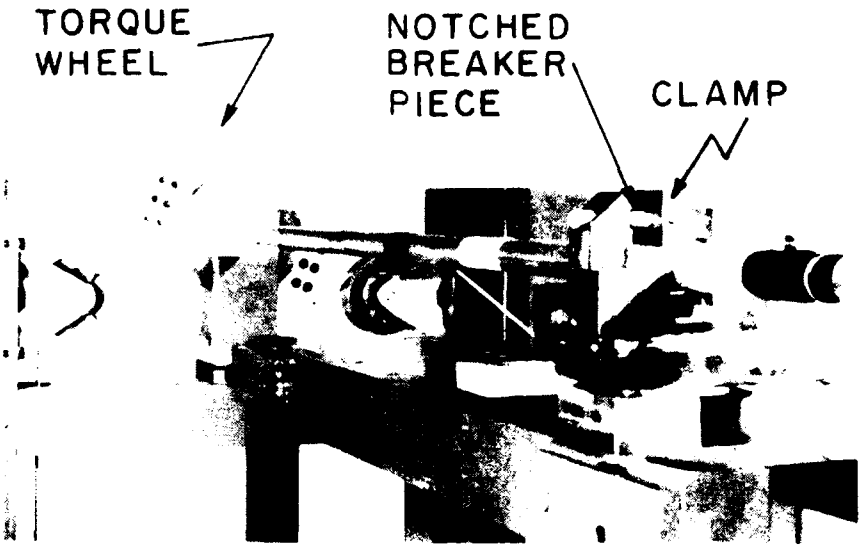

FIGURE 5.(A) TORSIONAL KOLSKY BAR SHOWING TORQUE WHEEL AND CLAMP.

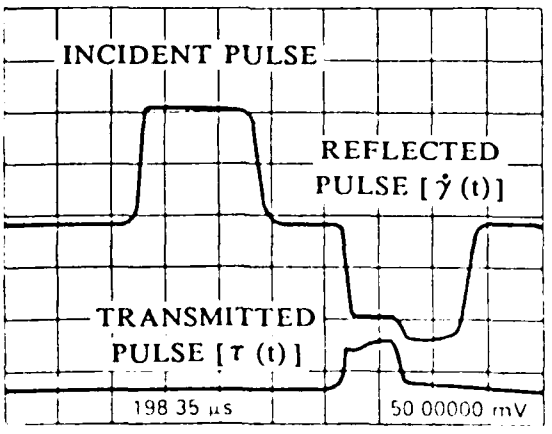

FIGURE 5.(B) OSCILLOSCOPE RECORD FROM A TEST WITH THE TORSIONAL KOLSKY BAR. EACH HORIZONTAL DIVISION EQUALS 200 µs. FRACTURE OF THE SPECIMEN CAUSES THE MAGNITUDE OF THE TRANSMITTED PULSE TO DROP TO ZERO.

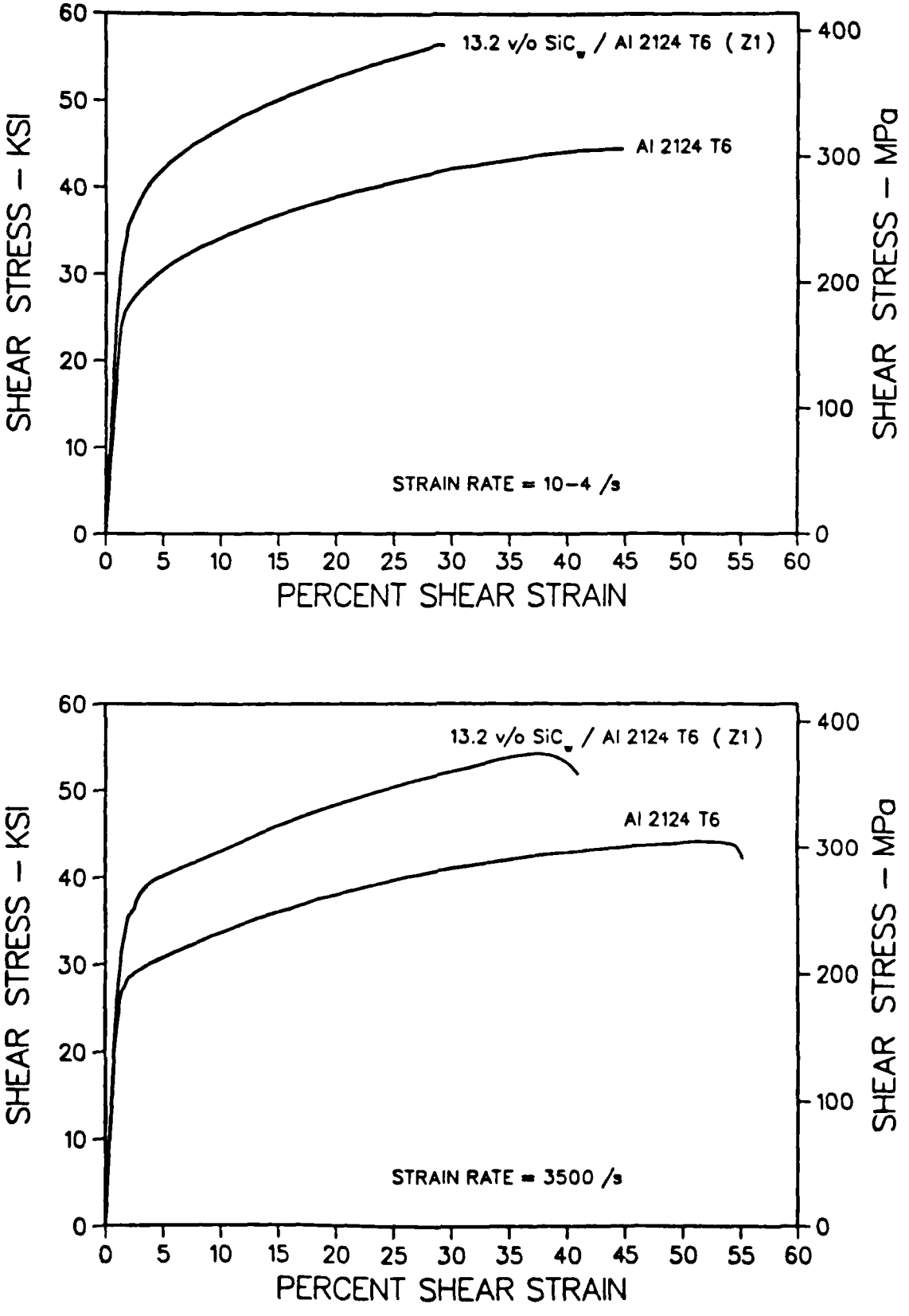

FIGURE 6. QUASI-STATIC AND DYNAMIC STRESS-STRAIN BEHAVIOR IN SHEAR COMPARING REINFORCED AND UNREINFORCED MATERIAL.

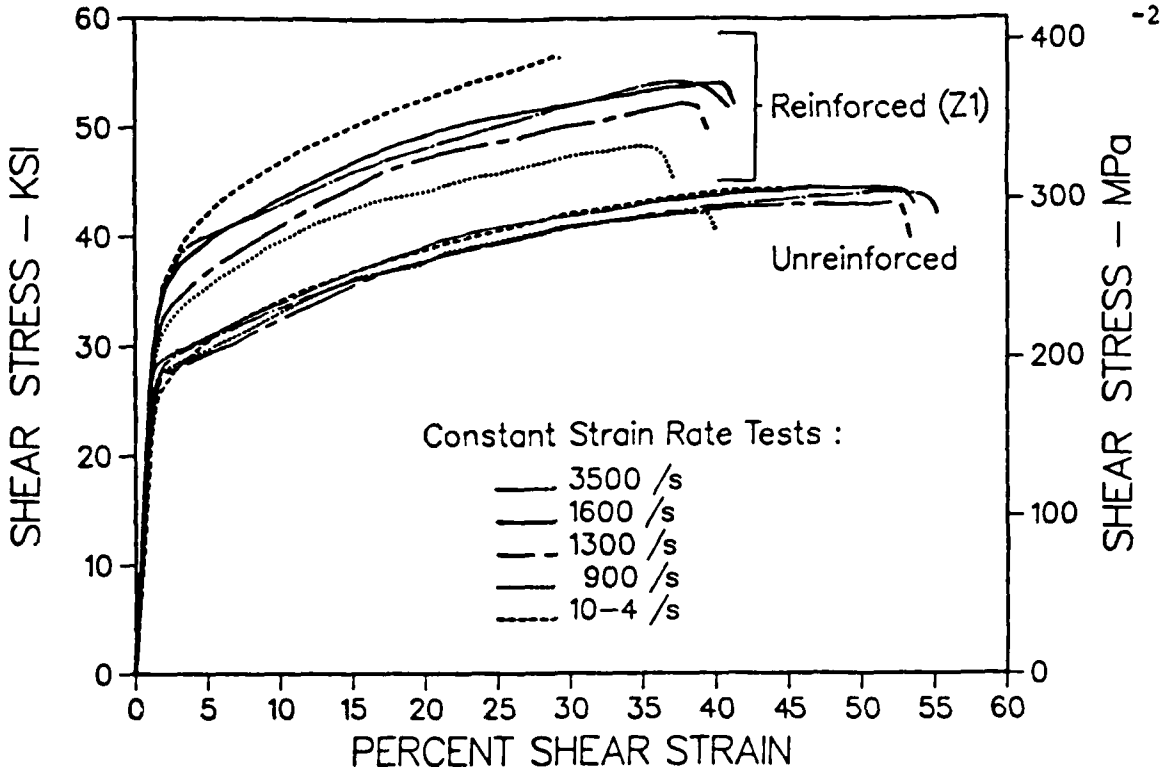

FIGURE 7. INFLUENCE OF STRAIN RATE ON STRESS-STRAIN BEHAVIOR IN SHEAR FOR 2124-T6 ALUMINUM ALLOY REINFORCED WITH 13.2v/o SiC_w (SPECIMEN Z1) AND UNREINFORCED.

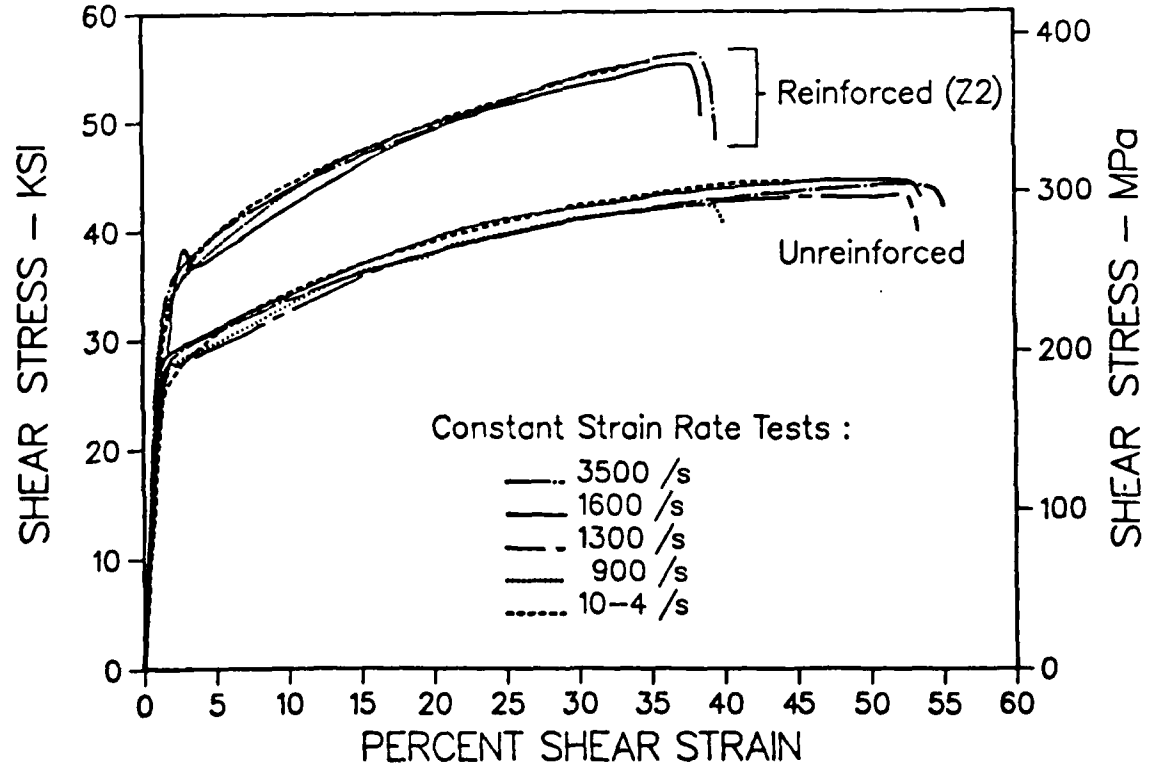

FIGURE 8. INFLUENCE OF STRAIN RATE ON STRESS-STRAIN BEHAVIOR IN SHEAR FOR 2124-T6 ALUMINUM ALLOY REINFORCED WITH 13.2v/o SiC_w (SPECIMEN Z2) AND UNREINFORCED.

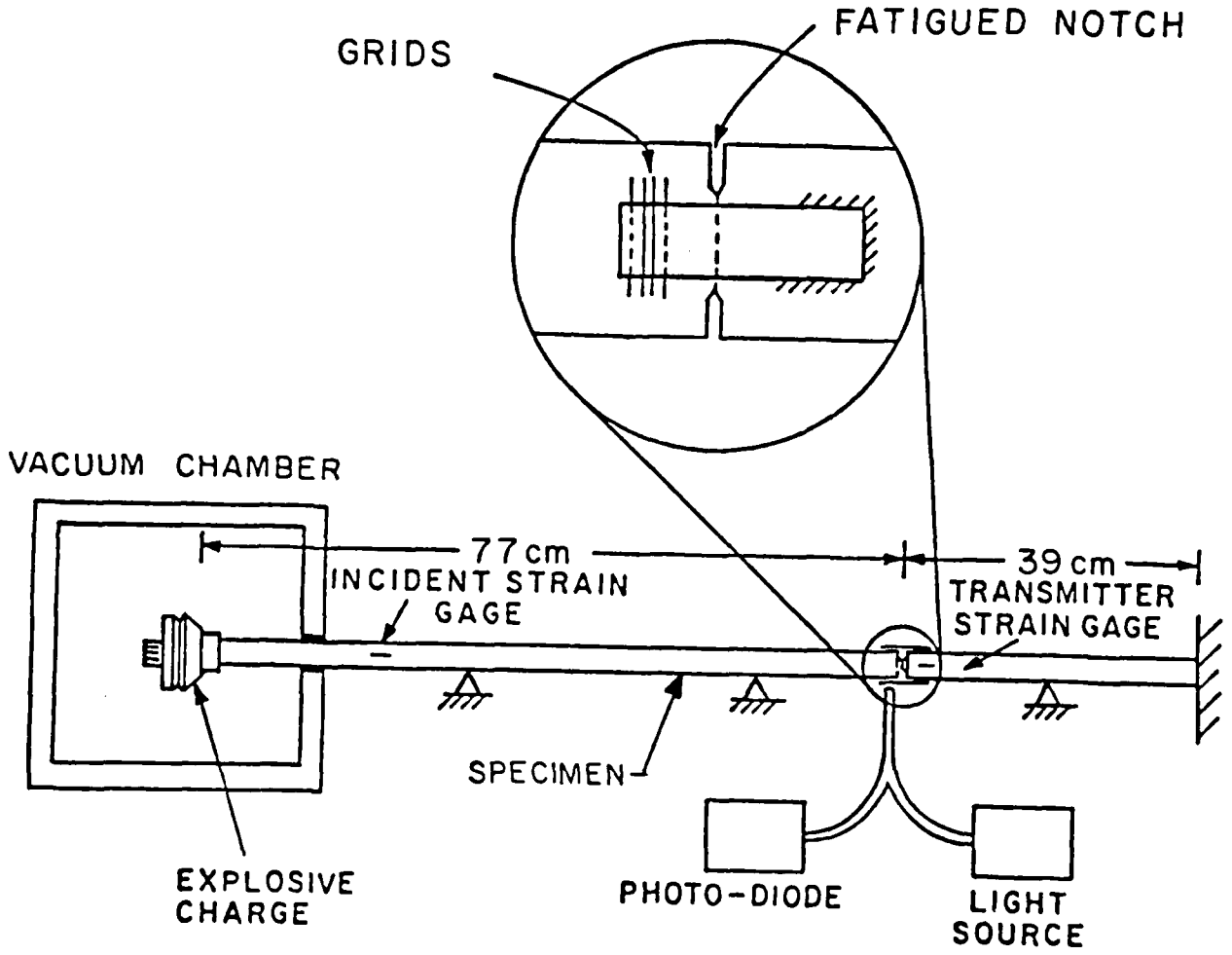

FIGURE 9. SCHEMATIC DIAGRAM OF APPARATUS FOR DYNAMIC FRACTURE INITIATION EXPERIMENT USING NOTCHED ROUND BAR. DETONATION OF THE EXPLOSIVE CHARGE INITIATES A TENSILE LOADING PULSE TRAVELING FROM LEFT TO RIGHT. THE INSET SHOWS DETAILS OF THE OPTICAL METHOD USED TO MEASURE COD.

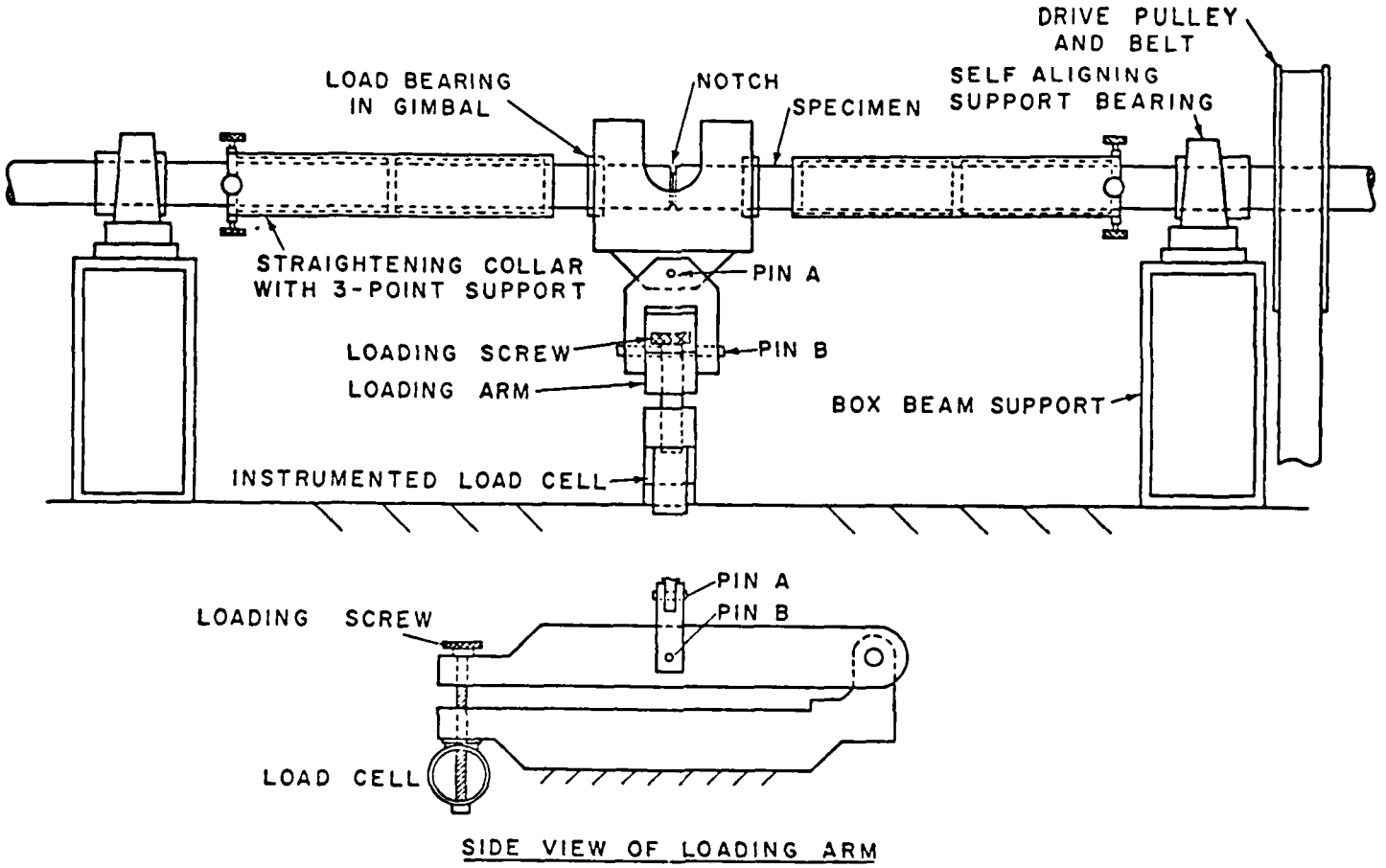

FIGURE 10. SCHEMATIC OF FATIGUE APPARATUS.

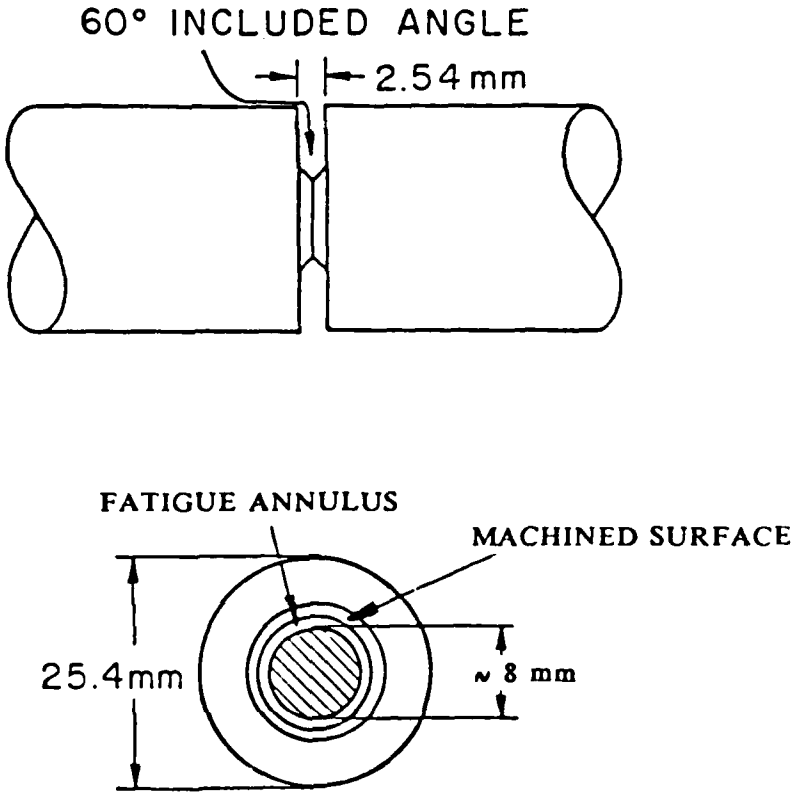

FIGURE 11. NOTCHED SECTION OF SPECIMEN SHOWING LIGAMENT REMAINING AFTER FATIGUE (NOMINALLY 8mm DIAMETER).

DYNAMIC FRACTURE TEST

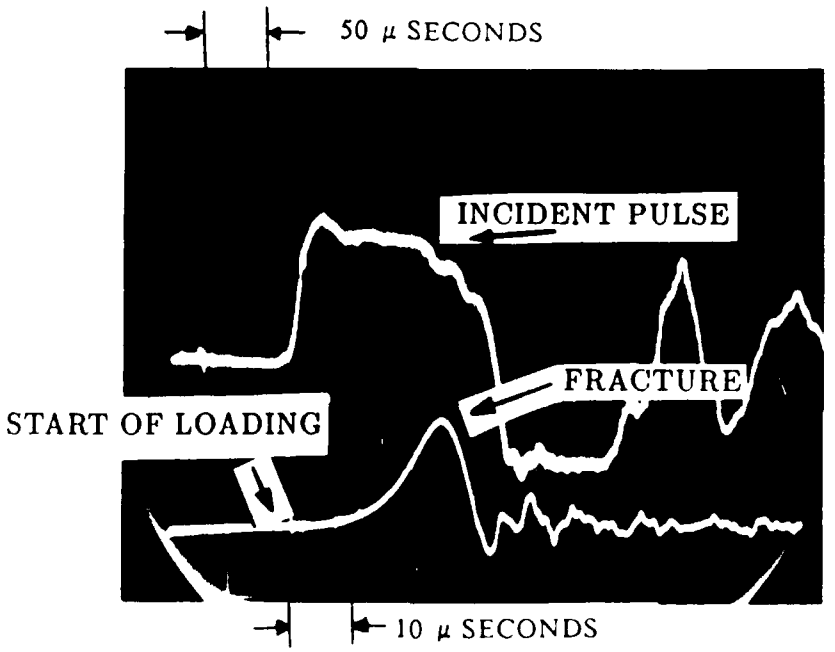

SPECIMEN NO: Z2

13.2 v/o SiCw / Al 2124 T6

FIGURE 12. PHOTOGRAPH OF OSCILLOSCOPE TRACES OBTAINED IN DYNAMIC FRACTURE TEST. UPPER TRACE SHOWS INCIDENT AND REFLECTED PULSES. LOWER TRACE SHOWS TRANSMITTED PULSE.

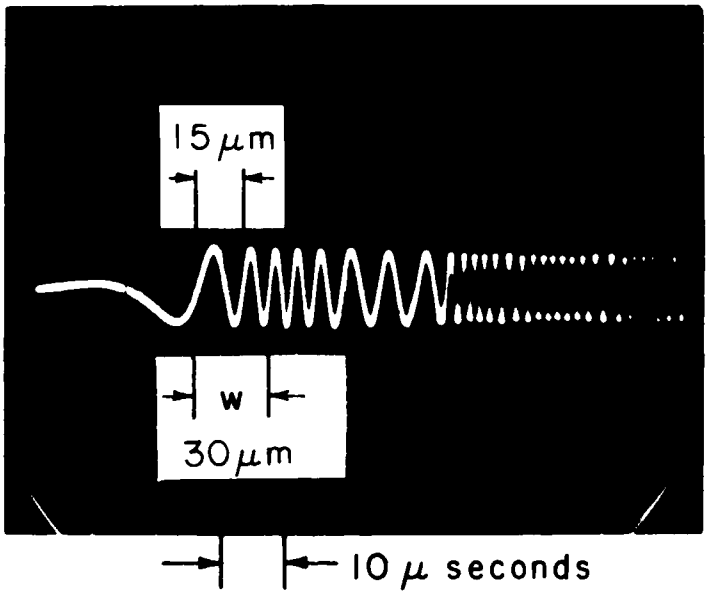

FIGURE 13. OSCILLOSCOPE PHOTOGRAPH SHOWING OUTPUT OF OPTICAL GRID SYSTEM. CORRESPONDING LINEAR DISPLACEMENTS ARE SHOWN.

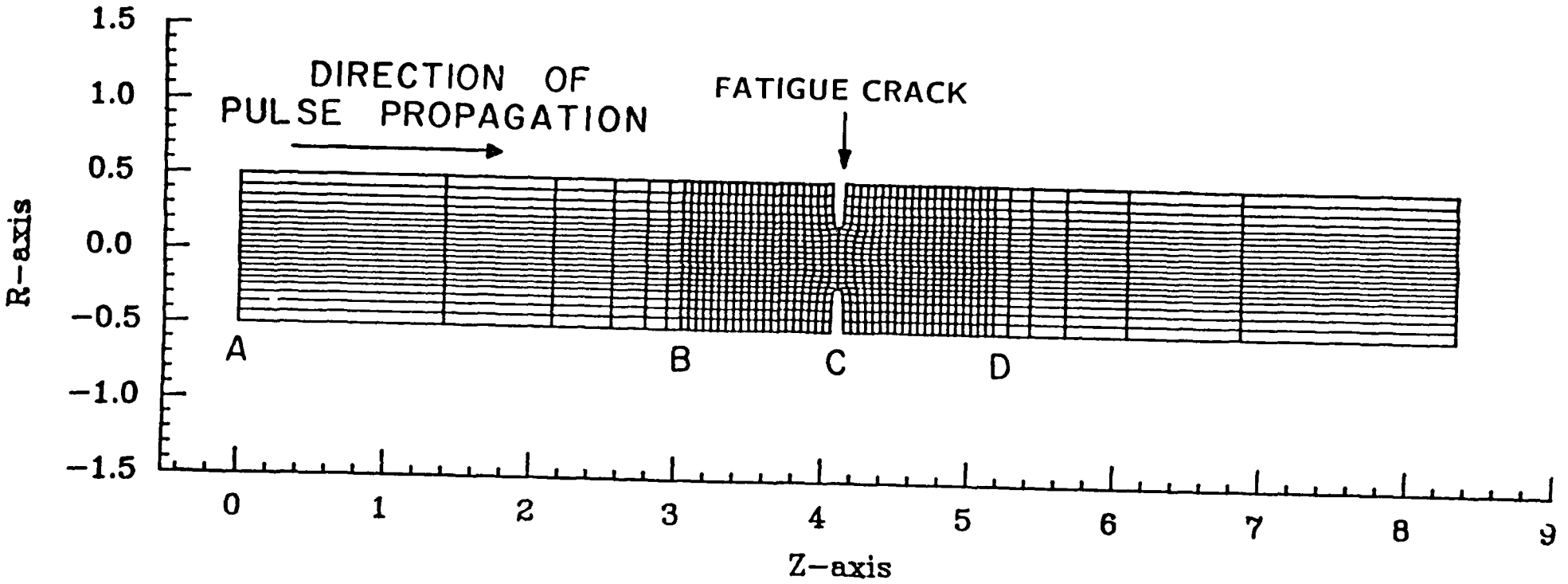

FIGURE 14. FINITE ELEMENT GRID USED IN THE WAVE PROPAGATION ANALYSIS OF THE FRACTURE INITIATION TEST. THE RESULTS OF THE ANALYSIS SHOW THAT AN ACCURATE VALUE OF J_{ID} IS OBTAINED AND THAT THE STRESS FIELD AT THE CRACK TIP IS MODE I UNDER PLANE STRAIN.

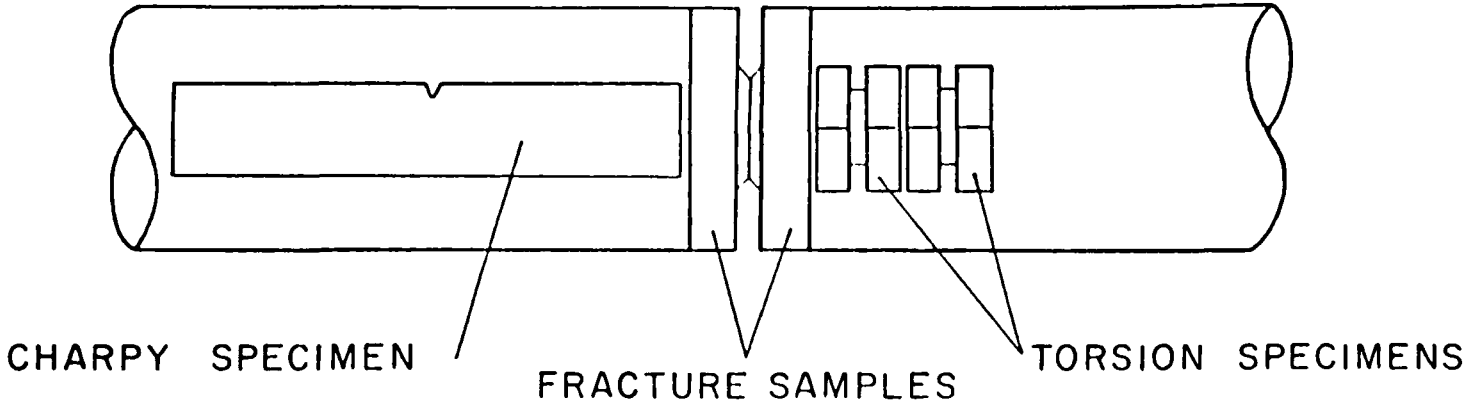

FIGURE 15. LOCATION OF THE MATERIAL FOR THE TORSION AND CHARPY SPECIMENS IN THE STATIC FRACTURE INITIATION SPECIMEN.

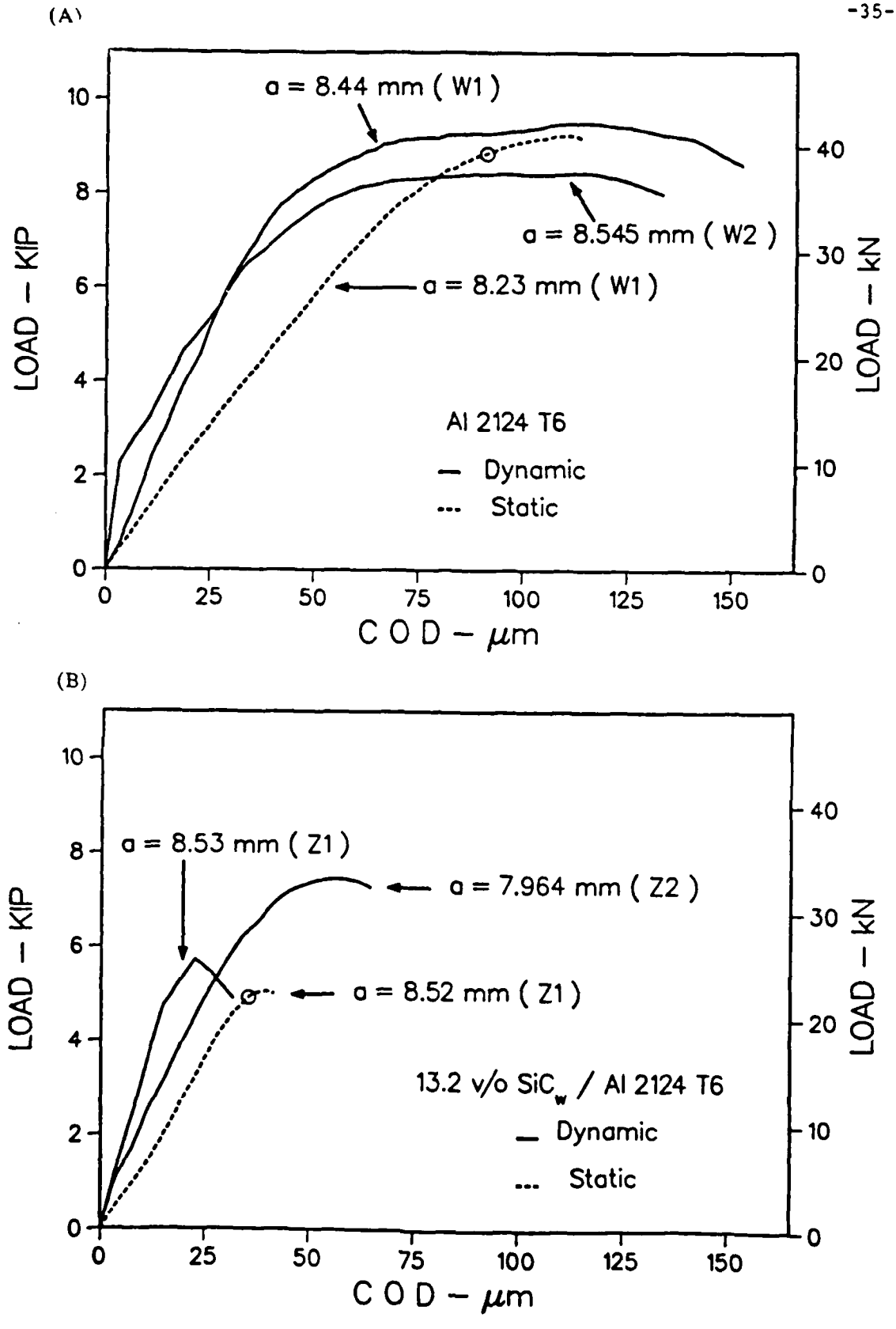

FIGURE 16. TYPICAL TEST RECORD OF LOAD AS A FUNCTION OF CRACK OPENING DISPLACEMENT FOR THE FRACTURE INITIATION TEST IN 2124-T6 ALUMINUM (A) UNREINFORCED AND (B) REINFORCED WITH 13.2v/o SiC_w.

(A)

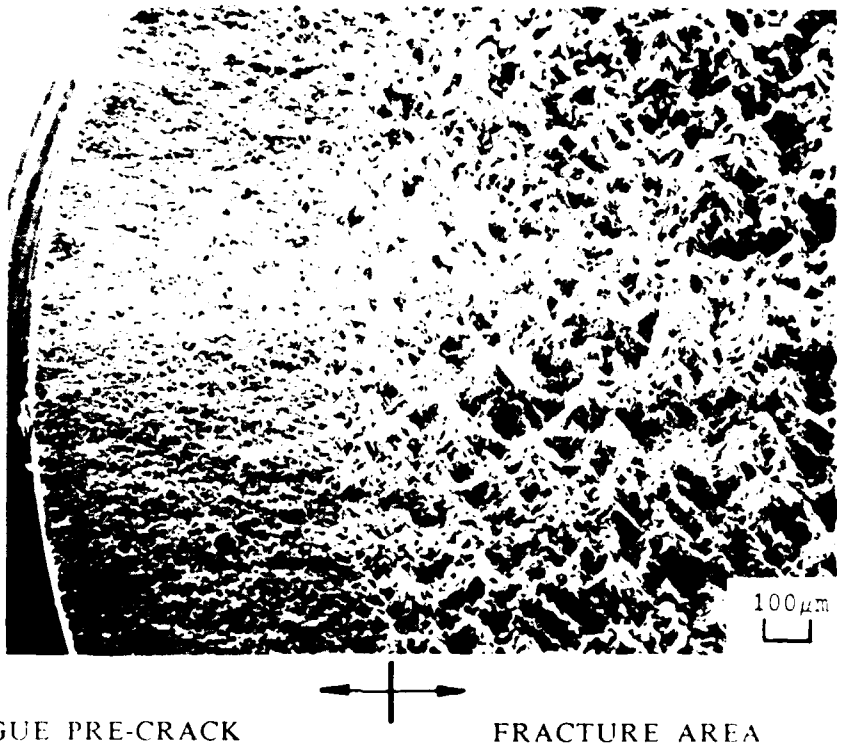

(B)

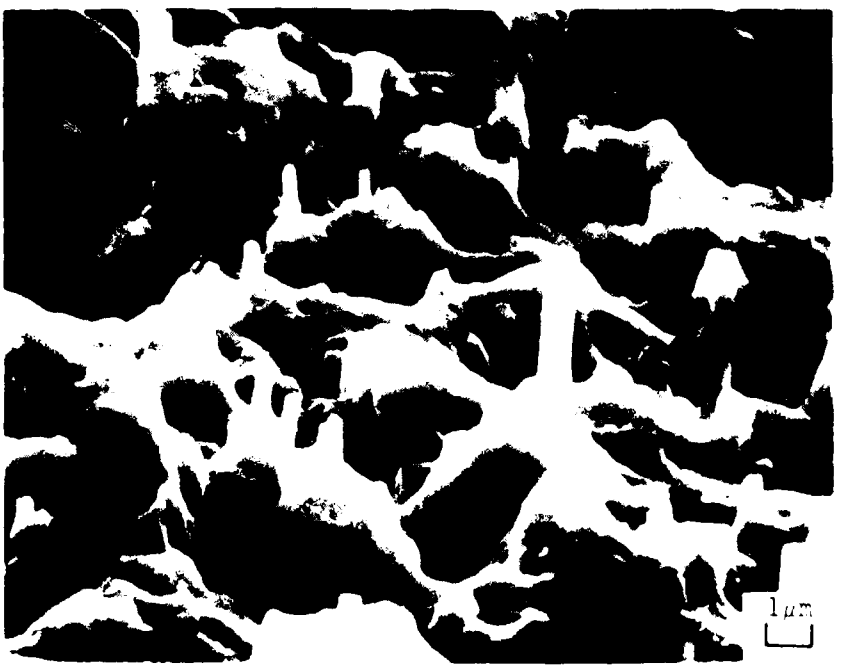

FIGURE 17: SEM FRACTOGRAPHS OF REINFORCED MATERIAL, (A) FATIGUE PRECRACK AND FRACTURE INITIATION AREAS AND (B) DETAILS WITHIN THE FATIGUE ANNULUS

(A)

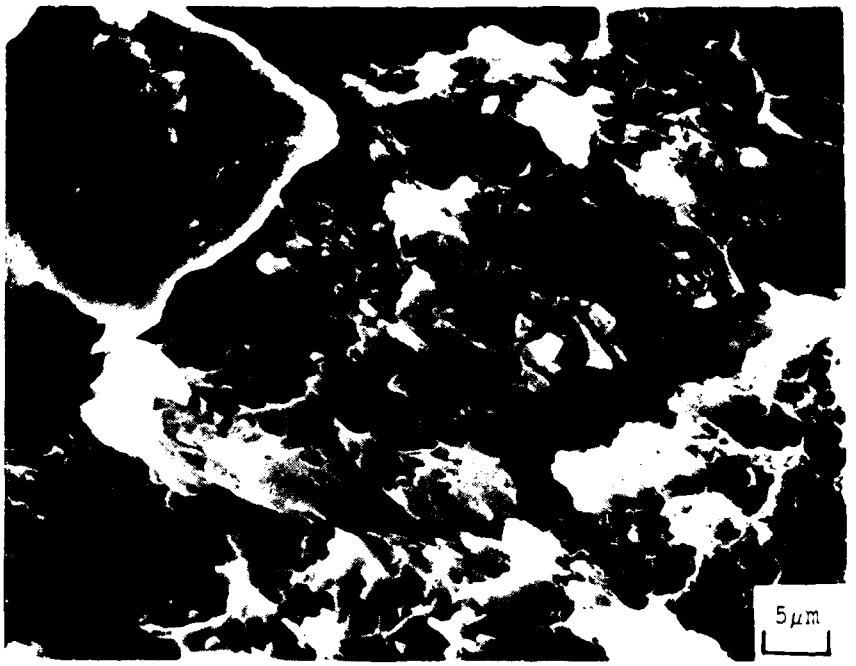

(B)

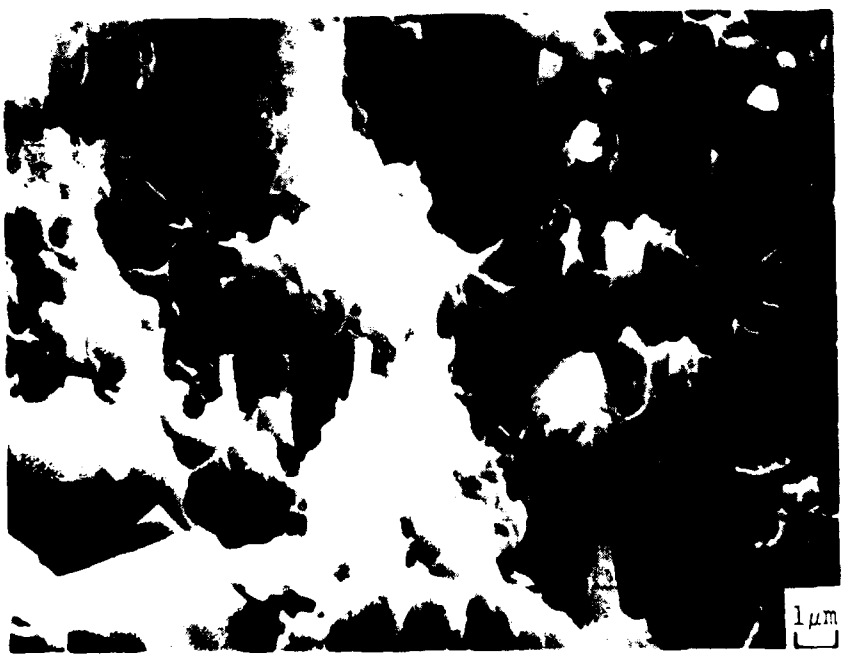

FIGURE 18. SEM FRACTOGRAPHS WITHIN FRACTURE INITIATION AREA AFTER DYNAMIC TEST WITH REINFORCED MATERIAL (A) NORMAL TO FRACTURE SURFACE AND (B) AT 45° TILT.

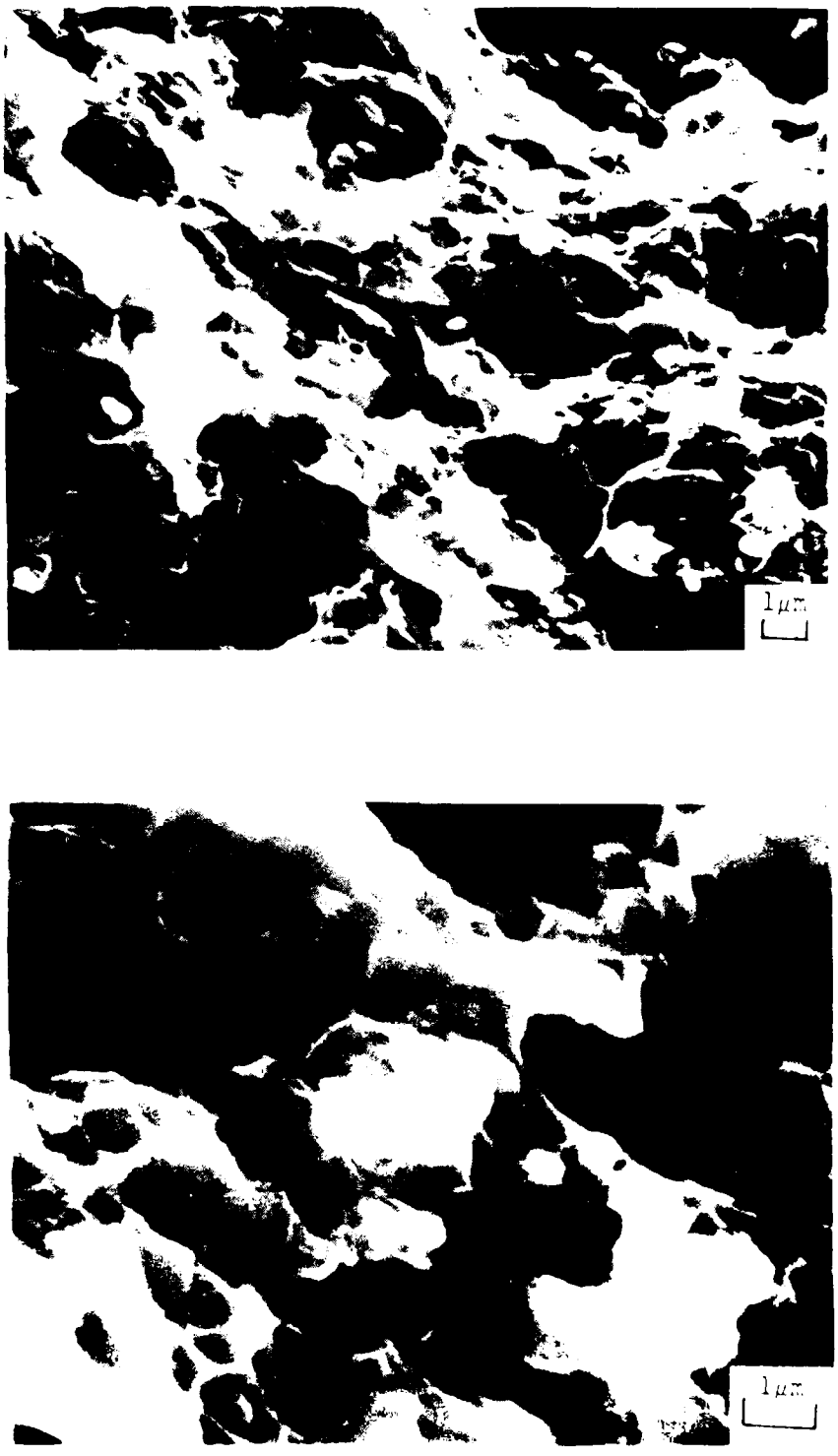

FIGURE 19. SEM FRACTOGRAPHS AFTER DYNAMIC TEST WITH REINFORCED MATERIAL. FRACTOGRAPHS ARE MADE IN AREA OF RUNNING CRACK BEYOND THE FRACTURE INITIATION AREA.

(A)

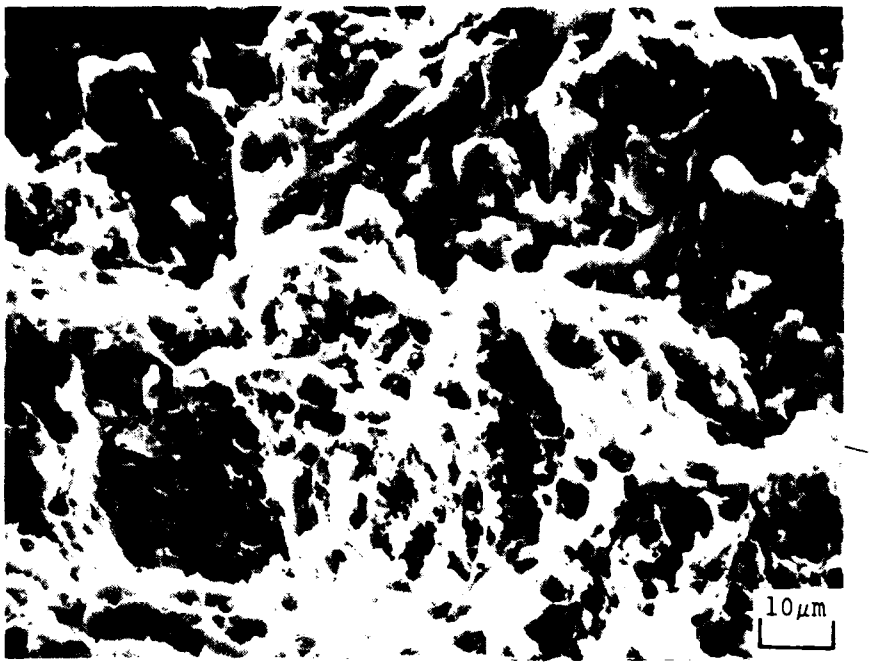

(B)

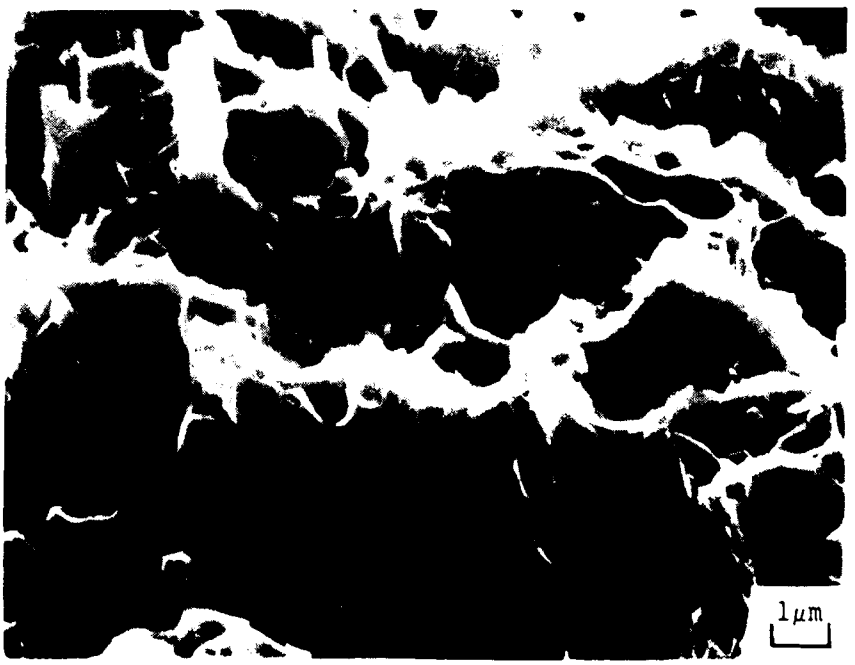

FIGURE 20. SEM FRACTOGRAPHS AFTER STATIC FRACTURE TEST WITH REINFORCED MATERIAL (A) FATIGUE PRE-CRACK AREA AT TOP AND FRACTURE INITIATION AREA AT BOTTOM OF PHOTOGRAPH, AND (B) DETAILS WITHIN FRACTURE INITIATION AREA.

END

4-[redacted]-87

DTIC